Proceedings of the ASME 2020
International Design Engineering Technical Conferences
and Computers and Information in Engineering Conference
IDETC/CIE2020
August 17-19, 2020, Virtual, Online

DETC2020-22753

DESIGN OF A LARGE WORKSPACE PASSIVE SPHERICAL JOINT VIA CONTACT EDGE DESIGN

Neil M. Bajaj & Aaron M. Dollar
Yale University
New Haven, CT

ABSTRACT

This paper presents the design of a compact ball and socket type spherical joint that makes use of passive elements to increase the range of motion to greater than a hemisphere with infinite roll capacity. We discuss the limitations of typical spherical joints due to simple geometric considerations, and how the addition of redundancy, passive elements, and multiple contacting surfaces of differing geometry can increase the workspace of these joints. We discuss the relationship between kinematics, mechanical conditions (e.g. friction and contact forces) under quasistatic motion, and geometry required to achieve the increased range of motion. Furthermore, we provide a metric for assessing the viability or benefit of a potential design. Finally, we validate one of our designs with a physical prototype and demonstrate its achievable range of motion.

1. INTRODUCTION

Kinematically, a spherical joint is a type of kinematic device with three (generally) linearly independent axes of rotation intersecting at a common point. Physically, there exist multiple ways of implementing this type of joint, including traditional ball and socket joints, three serial revolute joints with common intersection axis (often called roll-pitch-yaw devices or similarly named), universal joints in series with a revolute joint, or through more complicated spherical mechanisms[1]–[5]. While many of these implementations have differing benefits depending on the application, in terms of compactness and simplicity, the ball and socket design tends to outperform the other types.

Passive spherical joints tend to be important components of spatial (i.e. nonplanar) mechanisms, especially when considering spatial parallel mechanisms. Parallel mechanisms are composed of a relatively fixed base and mobile platform, connected by a number of serial legs with varying mobility. In general, some of the joints in these legs will be passive (unactuated), and most of the actuated joints tend to be single degree-of-freedom (DOF) devices such as rotary or linear motors.

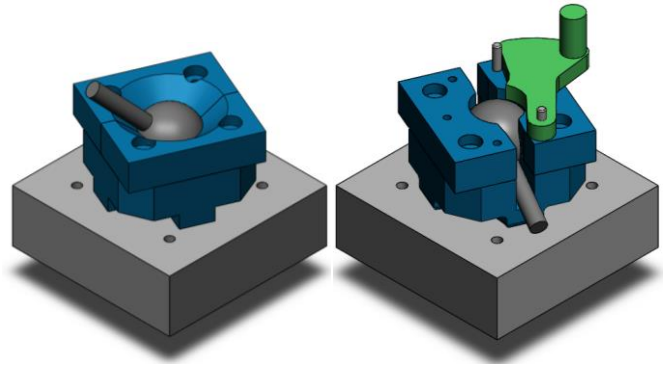

FIGURE 1: (Left) Typical ball and socket spherical joint with approximately 50º range of motion and infinite roll about shaft. (Right) An example of our proposed multiple contact edge ball and socket design, capable of 150º range of motion, with infinite roll about the shaft.

Passive spherical joints can provide the necessary mobility in the legs of high DOF parallel mechanisms, such as the Stewart platform [6], Delta Robot [7]–[9], or parallel wrist devices [10]. They can also serve to constrain other types of mechanisms to spherical motion, which sometimes are designated as wrist, ankle, hip or shoulder mechanisms due to the biological resemblance. However, the range of motion of a spherical joint can often be the limiting factor in the range of motion of the larger mechanism. Though some work considers the motion limits of passive joints within mechanism design, this is not always considered in kinematic design and optimization, though it must be considered in the physical design to prevent potential damage to the overall mechanism. We thereby assert that increasing the range of motion of spherical joints may increase the overall workspace of the mechanisms they constitute.

In this work, we propose the design of a ball and socket type spherical joint that can achieve a range of motion greater than a single hemisphere with infinite roll (rotation about the output shaft of the spherical joint) at any position in its workspace. Ball

and socket joints with a static socket typically cannot have a hemispheric range of motion, as doing so would imply that at least half of the socket was missing and the ball could simply fall or be pulled out under some particular forces. By including additional passive revolute joints (axes of which still intersect at the center of the ball), multiple potential contact surfaces (places where the output shaft may contact the socket, or "capture" housing), and elastic/deformable elements, we create a joint capable of greater than hemispheric motion.

The notion of using redundant joints and elastic elements is similar to the passive redundant spherical joint proposed in [11] though their design utilizes a yoke based universal joint with a revolute joint on both the base and output shaft. Theirs is the most comprehensive treatment of large range of motion passive spherical joint design the authors could determine, and they establish some principles to be used in the design herein. However, we believe our design may address some issues with [11]. Namely, a ball and socket joint can likely provide greater strength and stiffness than the yoke based universal joint. In the universal joint design, loads (including torsional and bending loads) are passed through the pins that correspond to axes of revolution in the joint. These can thus require bearings if the mechanism is to be used under load, and the yoke arms themselves must be sufficiently strong/thick to support the loads coming through the pins or bearings. However, the thickness of the yokes can limit compactness, and to a limited degree, the range of motion of their mechanism. In [12], a similar idea using ball and socket joints is shown, though no analysis or design is put forth.

The remainder of this paper is structured as follows. In Section 2, kinematic, geometric, and mechanical terminology and relevant concepts are introduced. In Section 3, our design is detailed and conditions for achieving a larger range of motion are discussed. In Section 4, we propose a metric for determining the efficacy of any particular design, and evaluate a few of our designs using this metric. In Section 5, we briefly validate some of our designs with physical prototypes. We end in Section 6 with a conclusion and discussion of future work.

2. KINEMATIC & MECHANICAL CONSIDERATIONS

Before moving on to more specific concepts, we begin by defining the physical components of the ball and socket spherical joint. First, we consider the *ball* portion to obviously be composed of a sphere, and the center of which all the principal axes of rotation intersection. Emanating radially out of the ball is the output shaft, subsequently just called the *shaft*. In typical ball and socket joints, the socket is the unmoving base which surrounds the ball, and has a spherical cavity removed from it which the ball contacts. In our case, the socket itself is allowed to rotate about a vertical axis which passes through the ball.

On the socket, there may be bodies which move in a predetermined way relative to the socket through some kinematic constraints. We call these bodies *auxiliary bodies*. This axis supports the socket through the *proximal bearing*. In some cases, we also include a bearing on the shaft which shares the same axis as the shaft, and we call this the *distal bearing*.

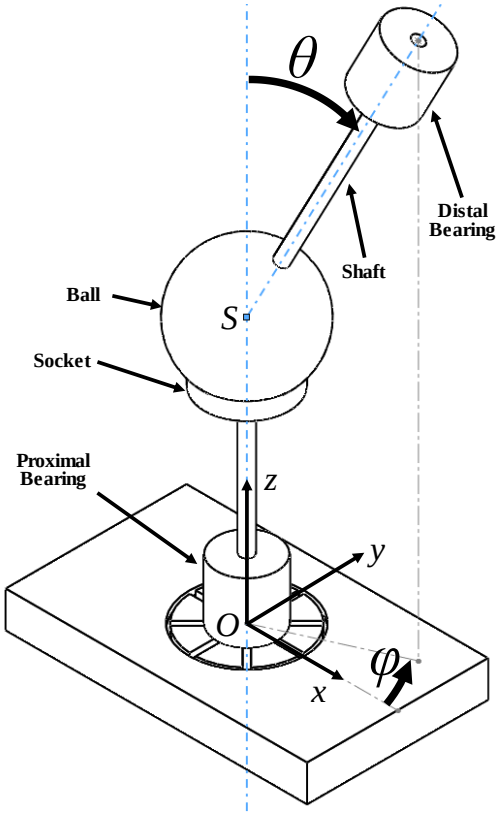

FIGURE 2: Kinematic representation of ball and socket spherical joint with additional passive joints. Relevant geometric and kinematic properties are shown.

Finally, we call the surface where the shaft may intersect the socket or the auxiliary bodies as the *contact surfaces*. For most of our analysis, we will actually be examining 1 dimensional *contact edges* rather than contact surfaces, but the shaft may in some cases be able to contact a 2D surface.

2.1 Kinematic Description

Fig. 2 shows a kinematic representation of the spherical joint design in consideration in this paper. The architecture of these joints can be represented as an RS, or sometimes RSR, serial chain, where the axis of rotation of the R joints intersect the center of the ball *S*. The socket can rotate about the first R joint, whose axis is the z axis, via the proximal bearing. In fig. 2, the socket is purposefully shown as a very small socket that would not retain the ball simply for illustration purposes, but in practice would surround the ball.

The output of at the end of the chain is either at the end of the shaft, rigidly fixed to the shaft if the architecture is an RS chain, or on the outside of the distal bearing if the architecture is RSR. The distal bearing shares its axis with the shaft axis, though its purpose will be discussed later. The origin *O* is fixed to the base, which is considered fixed in space. Either architecture constrains the output to spherical motion about *S*.

The angles θ and φ indicated in fig. 2 correspond to the polar and azimuthal angles, respectively. A third angle corresponding to roll about the shaft is not shown here, as majority of the

analysis is independent of this angle. The two relevant angles can thus be used to create 2D polar plots corresponding to the range of motion of a particular design, with polar angle as the radial coordinate and azimuthal angle as the angular coordinate on the plots.

2.2 Mechanical Considerations

2.2.1 Shaft Size Effects

Two important parameters in the design of ball and socket joints are the radius of the ball r_B and the radius of the shaft r_S. Without loss of generality, we may assume for the remainder of this paper that $r_B = 1$, and express the shaft radius r_S as a ratio of their radii, and thus partially nondimensionalize the analysis. We denote this ratio as r_T.

As described earlier, the socket has a spherical cavity in which the ball rests. To accommodate for the shaft, however, the ball must have an exposed area corresponding to a cutout portion of the socket, which must be a circle with diameter larger than that of the shaft to result in any motion. For symmetric ball and socket joints (with symmetry defined via a rotation about the vertical axis), the maximum cutout would correspond to a hemisphere of the ball revealed, as any larger than a hemisphere would cause the ball to fall out if it was pulled in the open direction. However, this is only the case for $r_T = 0$, as the shaft would contact the capturing portion of the socket before reaching $\theta = 90°$.

Moreover, an actual mechanical design requires more than an infinitesimal amount of capturing area on the ball, as tensile forces tending to pull the ball out could cause enough deformation to remove the ball from the only slightly capturing socket. Fig 3. shows the relationship between r_T, the capture overlap length d (defined in fig. 3), and the resulting maximum θ achievable. Note that the symmetry means the maximum θ is independent of φ.

Fig. 3 illustrates the limitations of typical symmetric ball and socket spherical joints. The available range of motion quickly falls even with rather small r_T. As a result, designs which are asymmetric about the vertical axis (i.e. with contact geometry that is a function of φ), one may potentially increase the range of motion, though capture overlap length must still be taken into account. If a mechanism requires only a long, thin band of spherical motion, then one may tailor the capture geometry and contact surfaces to be elongated in one direction and narrow in the orthogonal direction. This would form a cutout that would look much like a slot cut into the socket. Rod-end spherical joints typically employ this kind of capture geometry, though they are not capable of infinite roll, unless they make use of another R joint on the output, much like the distal bearing.

2.2.2 Contact Force Implications

As changing the geometry of the capture from a symmetric design to an arbitrary shape (as long as there is still some capture length), potentially with high aspect ratio, one may then attempt to leverage this large workspace in one direction (in a particular φ direction) to achieve a large workspace in all directions (for all φ). This is the purpose of the proximal bearing: to allow a range

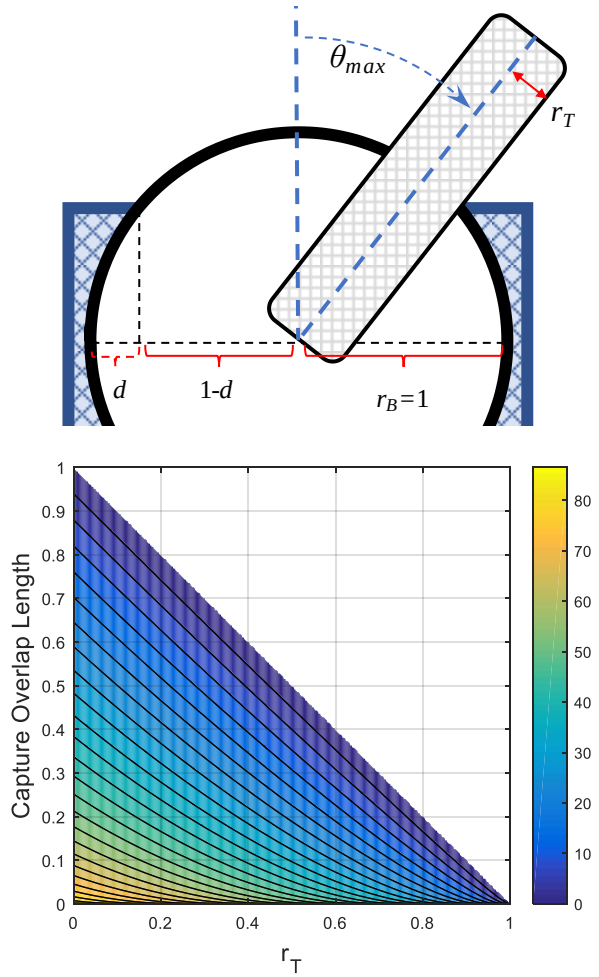

FIGURE 3: (Top) Cutaway diagram of ball and socket with shaft demonstrating capture overlap length d and its relationship to θ. (Bottom) Maximum allowable polar angle θ as a function of radius ratio r_T and d. The white area implies that the combinations of r_T and d would result in no range of motion, i.e. the shaft is too large for the desired amount of capture length.

of θ along a small range of φ to be applied to all φ. With the bearing, one could imagine changing the direction of large θ to align with the instantaneous direction of motion, i.e. aligning the slot with the intended direction of shaft motion. We call this alignment "reconfiguration," and it is formally constituted of a rotation of the ball and socket about the z-axis. While reconfiguration could likely be achieved through sensing, control, and actuation of the first R joint, we endeavor to find a completely passive solution.

During reconfiguration, we note that only the socket and potential auxiliary surfaces would be rotating about the z axis. The ball and shaft would still be moving in the same direction in the global frame that they were moving in before reconfiguration occurred.

To enable passive reconfiguration, we realize that reconfiguration need only occur when the shaft is in contact with a contact edge and trying to move into that edge. To formalize these notions, we define relevant contact quantities. Namely,

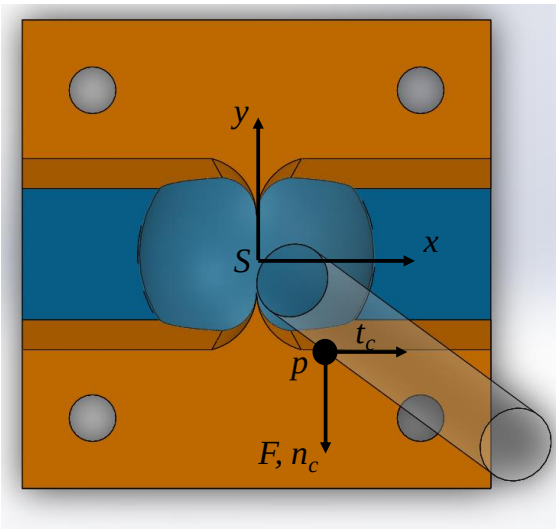

FIGURE 4: Depictions of the relevant contact geometry, projected into a plane normal to the z axis. Note that in the frictionless case, the contact force and contact normal must align, but in the case with contact friction between the shaft and contact edge, the frictional force may be a linear combination of tangent and normal vectors.

these are the contact location $\boldsymbol{p}$, contact normal vector $\boldsymbol{n_c}$, the contact tangent vector $\boldsymbol{t_c}$, and the contact force $\boldsymbol{F}$. See figs. 4, 5 for a geometric depiction of these quantities. In the frictionless case, $\boldsymbol{F}$ must align exactly with $\boldsymbol{n_c}$. With nonzero friction, $\boldsymbol{F}$ may be in the friction cone determined by the coefficient of friction between the shaft and contact edge of the socket, $\boldsymbol{n_c}$, and $\boldsymbol{t_c}$.

To simplify our discussion of the contact mechanics, we will project all of the relevant contact quantities into a plane normal to the z-axis and always passing through the actual 3D contact point. We call this plane the contact plane. While the z component of $\boldsymbol{p}$ may vary, all of our designs will generally ensure that $\boldsymbol{p}$ lies in one of two z planes, define either by the top of the socket or the top of an auxiliary body. We then disregard forces in the z direction and moments about the x and y axes, as well at the z component of the previously defined vectors, as they have little bearing on the reconfiguration mechanics.

Another simplifying assumption we make is the shaft's cross section, when projected into the contact plane, is always a circle with radius $\boldsymbol{r_T}$**.** While this would introduce larger errors at large $\boldsymbol{\theta}$, the near $\boldsymbol{\theta} = 0$

As the axis of the proximal bearing is in the z-direction, only the x and y components of the $\boldsymbol{F}$ and $\boldsymbol{n_c}$, are involved in the computation of the torque on the proximal bearing. We call this torque $\boldsymbol{M_S}$, as in the planar projection it is simply the moment about point $\boldsymbol{S}$. We can thus derive a condition for reconfiguration:

$$M_S = p_x F_y - p_y F_x \neq 0 \qquad (1)$$

In the frictionless contact case, this condition encompasses the fact that a moment must be generated to cause reconfiguration, and due to the reconfiguration corresponding to rotation about $\boldsymbol{S}$, (1) also corresponds to the way the surface must move to accommodate the desired shaft motion. This is because at points where no moment is created, this also corresponds to

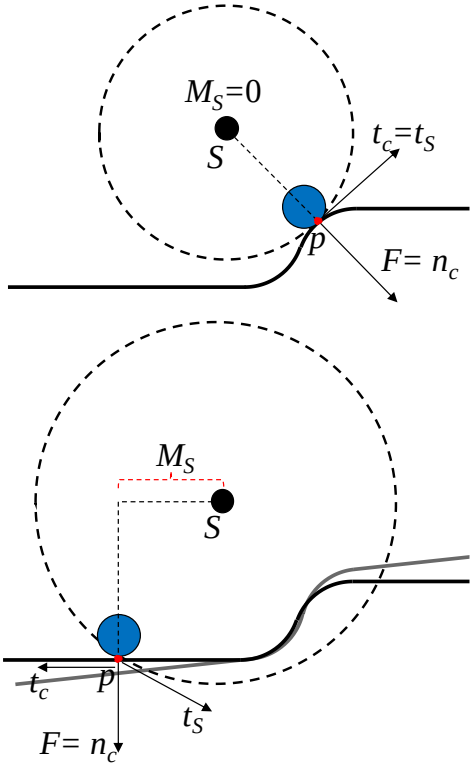

FIGURE 5: Conditions for reconfiguration to occur. (Top) The contact force induces no moment about $\boldsymbol{S}$, as its line of action passes through $\boldsymbol{S}$. Moreover, the circle tangent and contact tangent align, meaning there is no way for the shaft to move into the surface and p is singular. (Bottom) The contact force induces a CCW moment about $\boldsymbol{S}$, and the contact tangent $\boldsymbol{t_c}$ and a positive component of the circle tangent $\boldsymbol{t_S}$ span the all potential directions of motion into the surface. The light grey line corresponds to the way the contact edge would move post reconfiguration.

cases where reconfiguration would instantaneously not allow the shaft to move along its desired motion direction. We call any such point on the contact edge where this would occur a *singularity*.

Fig. 5 shows why this is the case. To demonstrate this, we must also define a new vector $\boldsymbol{t_S}$, corresponding to the motion of the contact edge if reconfiguration were to occur. We call $\boldsymbol{t_S}$ the *circle tangent*. This vector is located at $\boldsymbol{p}$, and is tangent to a circle centered at $\boldsymbol{S}$ and passing through $\boldsymbol{p}$. The direction of this tangent vector is dependent on the sign of the moment induced by the contact force. A counterclockwise $\boldsymbol{M_S}$ would result in $\boldsymbol{t_S}$ also being a counterclockwise tangent vector with respect to the aforementioned circle.

Assume $\boldsymbol{F} = \boldsymbol{n_c}$ (frictionless) and assume WLOG that the instantaneous desired shaft motion in the contact plane is also along the $\boldsymbol{n_c}$. This means the shaft is trying to move into the contact surface of the socket. In fig. 5 top, we see that not only would there be no moment to cause reconfiguration, but even if there was a moment, the contact edge would not move along the direction $\boldsymbol{n_c}$. In contrast, fig. 5 bottom shows a case where reconfiguration would indeed be possible as $\boldsymbol{M_S \neq 0}$, and where the induced reconfiguration would allow for the shaft to move

along the direction $\boldsymbol{n_c}$. The condition indicating that reconfiguration would allow motion into the surface is

$$a_1 t_c + a_2 t_S = n_c \qquad (2)$$
$$a_2 \geq 0$$

Because by definition $\boldsymbol{t_c}$ is always normal to $\boldsymbol{n_c}$, the only way Eq (2) is not satisfied is when $\boldsymbol{t_S} = \boldsymbol{t_c}$. This can only occur when the line of action of $\boldsymbol{n_c}$ passes through $\boldsymbol{S}$ and $\boldsymbol{p}$ is a singularity. Thus, Eq (1) and (2) state the same condition in the frictionless case. This also shows that a reconfiguring spherical joint with a single contact edge cannot be "self-locking," i.e. it cannot produce a moment that would oppose its direction of intended motion if there is only a single contact.

2.2.3 Frictional Issues

So far, we have assumed that friction between the shaft and the contact edge, between the ball and socket, and in the proximal bearing are all 0. When any one of these assumptions in not met, the mechanics may change slightly. The first two conditions can partially be mitigated by use of the distal bearing, whereas the third condition imposes a change to Eq. (1). We assume a Coulomb friction model in general.

Firstly, if friction between the shaft and contact edge is high, a few implications arise. Firstly, $\boldsymbol{n_c}$ and $\boldsymbol{F}$ may no longer align, and the constraint would then be that $\boldsymbol{F}$ must lie within a friction cone defined by $\boldsymbol{n_c}$ and a coefficient of friction. Furthermore, this may mean that moments due to frictional force are induced. However, one may still determine the contact force F using the desired shaft motion if static and the Maximum Dissipation Principle [13] when sliding. To avoid considering the intended direction of motion, we may instead assume the worst-case scenario: if any force within the friction cone does not induce a moment, then the socket will not reconfigure, and this contact point is a singularity. This is a conservative assumption, but can serve as proof that a particular contact edge design could have an entire singular zone.

To mitigate this condition, if we were to allow the shaft to roll along the contact surface, then we would not need to consider sliding friction. We can do this by decoupling the roll of the shaft from the roll of the output, which is the purpose of the distal bearing. In this case, the ball is rolling relative to the socket, even if reconfiguration is not occurring.

On the other hand, if the contact friction is low, but the friction between the ball and socket is high, this would mean reconfiguration would have to overcome the friction between the ball and socket, as the ball stays relatively fixed in roll during reconfiguration. Again, the distal bearing can alleviate this issue by allowing the ball to roll very little or not at all within the socket, and then allow the shaft to slide over the contact edges. The output can then still be independent of this fixed and force dependent roll.

However, if both the contact friction and friction due to the ball are high, one would need to place another bearing on the shaft to interact with the contact edge. That bearing would then roll along the contact edge or reduce friction along the contact edge while allowing the ball and shaft to roll together with the socket. The distal bearing would then still decouple this roll from roll of the output. However, it may be difficult to fit a bearing on the shaft between edges, as this exacerbates the radius effects shown in fig. 3.

Finally, friction in the proximal bearing subtly affects reconfiguration. Instead of requiring $\boldsymbol{M_S}$ to be nonzero in Eq (1), we would instead require that its magnitude be greater than the bearing friction $\boldsymbol{M_B}$.

Depending on how $\boldsymbol{M_B}$ is modeled, different conditions of reconfiguration may arise. If we assume that $\boldsymbol{M_B}$ is a constant, regardless of the load, then the $\boldsymbol{M_S}$ simply needs to be greater than that value. This would require the geometry to be fully dimensionalized and actual value of the contact force to be determinable or known apriori to compute if reconfiguration would occur. This is because lengths and forces actual values with units must be known to compare them to torques, i.e. there is no way to dimensionlessly compare torques and moments. This case is representative of a ball bearing with roller elements used as the proximal bearing.

One may also consider the effect of choosing a plain bearing or bushing as the proximal bearing. These might be used over a bearing for many reasons, including size, cost, and complexity requirements. While some bushings are lubricated and behave similarly to bearings, at low forces, they may behave like surfaces with low coefficients of friction, admitting a Coulomb friction model. Using this kind of model for $\boldsymbol{M_B}$ leads to quite an interesting geometric interpretation. Firstly, the contact force $\boldsymbol{F}$ becomes proportional to the moment $\boldsymbol{M_B}$, as linearly increasing the contact force also linearly increases force through the bearing, and thus also the moment $\boldsymbol{M_B}$. This means we do not have to consider the magnitude of either the contact force or induced frictional moment, and can thus nondimensionalize the problem again. We consider all contact forces to be unit forces, and instead of using $\boldsymbol{M_B}$, we can consider the lever arm of $\boldsymbol{F}$ to be the quantity of interest. We then call the minimum lever arm that could cause reconfiguration $\boldsymbol{r_m}$**.** Qualitatively, the condition for reconfiguration becomes: if a contact force $\boldsymbol{F}$ or its line of action pass through a circle of radius $\boldsymbol{r_m}$ centered at $\boldsymbol{S}$, then reconfiguration will not occur. We define the actual contact force lever arm as radius $\boldsymbol{r_f}$. If we assume the frictionless contact case again, this becomes:

$$r_f = \left| p_x n_y - p_y n_x \right|_2 \geq r_m > 0 \qquad (3)$$

Eq (2) is fully contained within this constraint as long as the radius $\boldsymbol{r_m}$ is nonzero.

To keep the problem most general, we address this case and motivate the reason for our design. If a contact edge is continuous and has two sets of contact points, one set which causes a positive $\boldsymbol{M_S}$ and the other set a negative $\boldsymbol{M_S}$, then there must be at least one singularity on the surface. In addition, every point between regions where $\boldsymbol{M_S}$ has different sign is a singularity, and will not cause reconfiguration. If one applies Eq. (3) as the condition for reconfiguration, then there exist singular zones where no reconfiguration will occur.

We address this issue by introducing mobile auxiliary edges, which are connected to the socket but may move in some prescribed manner relative to the socket. Contact may transition

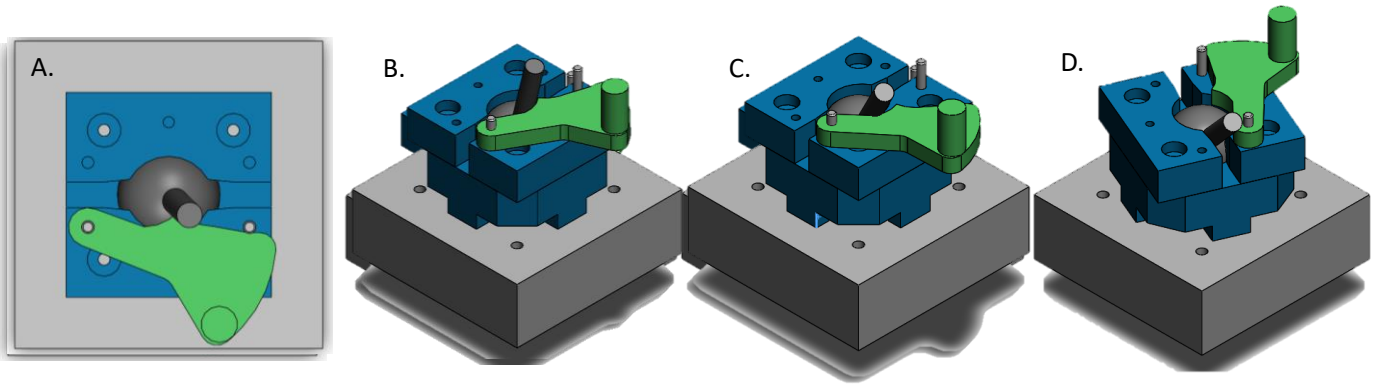

FIGURE 6. Operation of a multiple contact edge design. The blue pieces correspond to the socket, which can rotate about a bearing hidden in the grey base, and the green is the auxiliary body. Springs and additional hardware are suppressed for clarity. A. Top down view of multiple contact edge design. B. The shaft initially contacts the auxiliary surface, but the moment is not yet high enough to cause reconfiguration (contact point is in the singular zone). C. The shaft continues to move, further displacing the auxiliary body via rotation about its pivot pin. D. The moment becomes high enough and the socket rotates to clear a path for the shaft, allowing it to descend in the desired direction. The auxiliary body is restored to its initial position relative to the socket.

from one contact edge to another, which thus changes the direction of $\boldsymbol{n_c}$ and may be able to then induce a moment.

3. MULTIPLE CONTACT EDGE DESIGN

We now introduce our multiple contact edge design (fig. 6). The operating principle behind multiple contact edges is for the shaft to initially be in contact with a contact edge, preferably a contact edge belonging to an auxiliary body. If the moment induced by this contact is enough to cause reconfiguration, then the joint reconfigures and the auxiliary body stays fixed w.r.t. the socket. However, if the moment is not great enough, the auxiliary body will then move relative to the socket in a prescribed manner, either constrained by kinematics or elastic elements. This motion can generally change the contact location $\boldsymbol{p}$ and normal $\boldsymbol{n_c}$. If the shaft remains in contact with the contact edge on the auxiliary body and the reconfiguration condition is satisfied, then reconfiguration will occur.

If reconfiguration does not occur while the shaft is displacing the auxiliary body, eventually, another contact will appear between the shaft and a different auxiliary body or the socket's contact edge. If the "stiffness" of the new contact edge is higher than that of the previous one, increasing the contact force will generally tend to load the new contact edge more than the old one, causing the induced moment to change.

If reconfiguration did not occur during the initial contact with the auxiliary body's contact edge, we may say that contact occurred within the auxiliary body's singular zone. If, while in contact with the first auxiliary body, contact occurs on another contact edge, but outside of the new edge's singular zone, then reconfiguration will occur.

To narrow down the space of potential designs, we establish a number of criteria for the auxiliary bodies and contact edges:

1) We use a discrete rotational symmetry about the z axis for all contact edges of degree 2. This means that opposite sides are flipped mirror images of each other, and that there are only two sides
2) We only use two contact edges per side of the joint, one corresponding to the mobile auxiliary surface which moves relative to the socket, and one corresponding to the contact edge of the socket.
3) The auxiliary bodies rest on top of the socket in the z direction, and are planar regions extruded in the z direction. The tops of the sockets are also flat.
4) Any contact edge must be continuous and have a radius of curvature larger than the shaft radius. This prevents multiple contacts on a single contact edge, thus the contact force and resulting moment can be determined easily.
5) The auxiliary bodies must move in a planar fashion atop the sockets. Moreover, they must move on a single DOF trajectory in *SE(2)*, the space of rigid body motions in a plane.
6) The auxiliary bodies are "restored" to their original positions when they are unloaded through some elastic mechanism (springs, bands, etc.). This imparts the contact edge on the auxiliary bodies a prescribed stiffness.
7) Assume the socket is infinitely stiff.

These assumptions facilitate the design of auxiliary bodies and the way they move, but may exclude more optimal designs. For example, criteria 5 results in predictable motion, but if the contact edge on the auxiliary body was allowed to, for instance, pivot about different points depending on contact location, this may result in a design where singular zones do not meet.

Note that criteria 4 does not imply that there may not be multiple simultaneous contact locations on different contact edges, just that a single edge may not have multiple contact locations.

In our designs, if the shaft is not near a maximum of the range of motion, we enforce that contact first begin on an auxiliary body. As the auxiliary body is deflected (if the joint did not reconfigure), eventually, the socket contact edge would be contacted as well. Because the contact force on the auxiliary body is defined by a spring potential (i.e. a kinematic relationship), then the contact force on the auxiliary body's

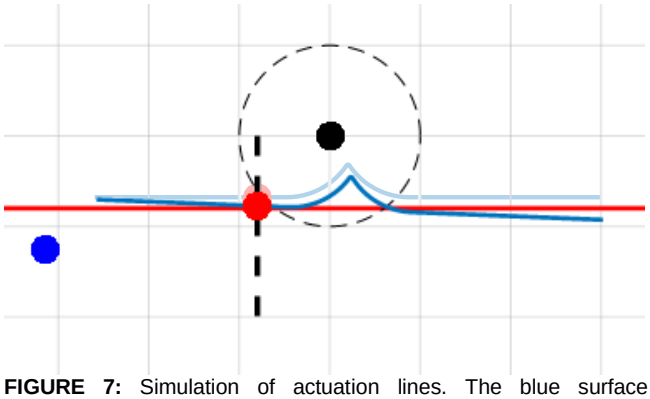

FIGURE 7: Simulation of actuation lines. The blue surface corresponds to the auxiliary surface's contact edge, which is able to pivot about the blue point. The solid red line is the socket's contact edge. The red point corresponds to the intersection point between the shaft and the contact edge. Note the pale blue line and pale red dot correspond to the aux. body's contact edge and the contact point before the aux. body deflected. Note that this pivot and geometry correspond to the joint design shown in fig. 6.

contact edge will not increase. However, the force on the socket's contact edge could increase even without any motion or reconfiguration due to its infinite stiffness. This situation could arise if the mechanism containing this spherical joint was subject to a position controller with Integral-like terms. In short, this implies that in the limiting case of large contact force after the auxiliary body "bottomed out," the resulting moment $\boldsymbol{M_S}$, or lever arm $\boldsymbol{r_f}$, appears to be completely a function of the geometry of the socket's contact edge, not the auxiliary body's contact edge.

We further only consider auxiliary bodies whose displacement profiles correspond to rotations about a fixed point, or deformable bodies that approximate rotation about a fixed point. We examine this particular class of bodies because they can be implemented quite compactly and with low additional friction in their motion, and are simple to return to their initial positions.

4. EVALUATION

4.1 Metric Description

To evaluate the efficacy of a potential design satisfying the criteria list in Section 3, we first develop a metric as to how much a particular design may alter effective lever arm $\boldsymbol{r_f}$, if reconfiguration were prevented by an external locking method. We call this metric the "arm increase" $\boldsymbol{g}$. Specifically, g is defined as the maximum increase in the lever arm $\boldsymbol{r_f}$ that would be achieved if the shaft desired motions were straight lines. These straight lines can be lines purely in the y direction, i.e. across the slot, (lines of constant x). We call these lines actuated lines, and could generally be in any direction. One such actuation line is the black dashed vertical line seen in fig. 7. Other actuation lines would be parallel to this one.

An immobile contact edge like the one on the socket will generally have only one contact edge per actuation line. However, as the auxiliary surface may continuously deflect, there are a series of potential contact points for each actuated line

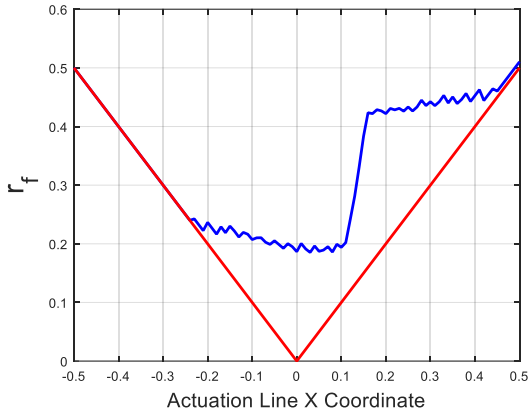

FIGURE 8: Socket contact edge $\boldsymbol{r_f}$ and max contact force along actuation line. The difference between the two lines is g. The sharp increase in the blue curve is due to the contact points cresting the peak seen in fig. 7.

(Fig 7). As a result, we compute $\boldsymbol{g}$ as the maximum moment arm that occurs on a given actuated line, whether it occurs on the auxiliary body's or the socket's contact edge.

Fig. 8. Shows a plot from which we may infer $\boldsymbol{g}$. Namely, we see the blue line which shows the maximal moment arm encountered along an actuation line. The red curve corresponds to the moment arm imparted by the socket alone. The difference between the two of these curves is $\boldsymbol{g}$ (as a function of the x coordinate). One may average $\boldsymbol{g}$ across all actuation lines to determine an average score for the entire design.

As a further heuristic check, one may observe the induced moment as a function of contact location (fig. 9). The dark blue

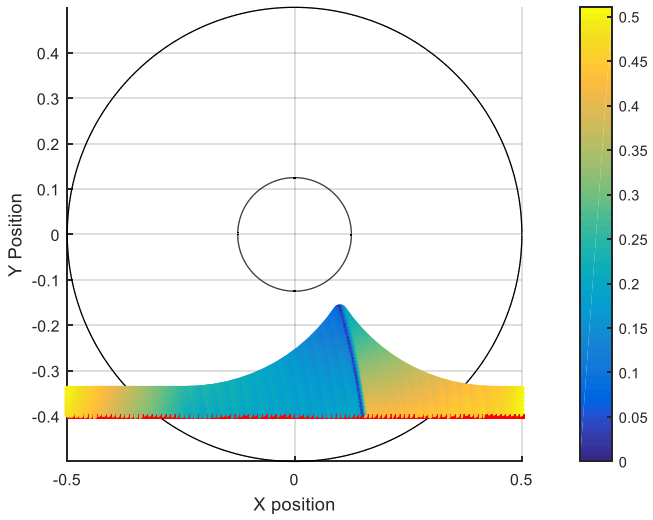

FIGURE 9. The moment arm $\boldsymbol{r_f}$ as a function of contact point. The unit circle is shown to indicate the ball, whereas the smaller circle indicates the shaft size. The red line corresponds to the contact edge of the socket, which is fixed and thus immobile and the limit of motion in the y direction The dark blue curve corresponds to the path of the singularity on the contact edge as the auxiliary body deflects about its pivot point located at (-1.5, -.0.62). As the singularity of the socket is at (0, -0.4), if $\boldsymbol{r_m}$ is low enough, this design will be able to reconfigure to maximum $\boldsymbol{\theta}$ in all directions.

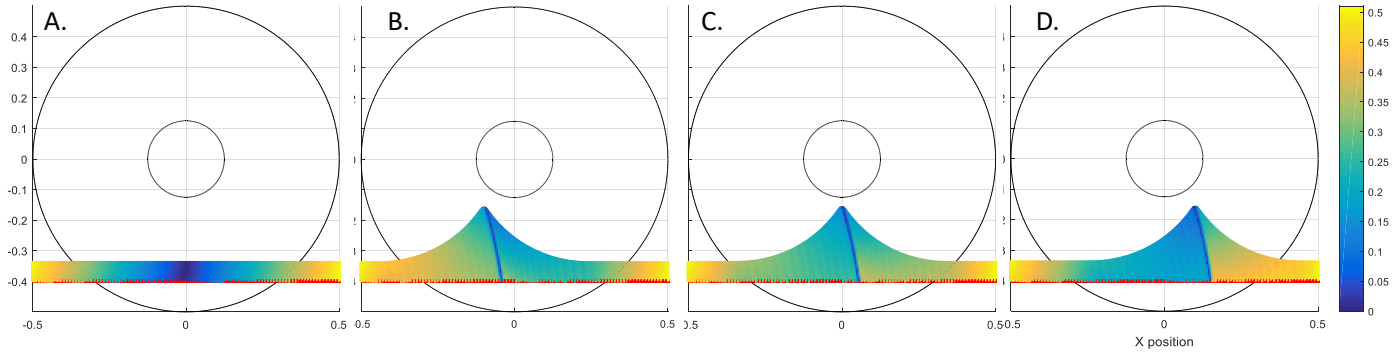

FIGURE 10. Comparison of r_f of different auxiliary body contact edges. The contact edge in the undeflected case corresponds to the outermost edge of the colored region, and as it is deflected, it sweeps out the rest of the colored region. The dark blue regions correspond to the singularity points / zones. A. Flat contact edge design. B. Peak design shifted left 10% (0.1). C. Peak design centered. D. Peak design shifted to the right 10%. Note that the pivot point of the deflecting surface is the same across all the displayed designs, but the singularity position on the auxiliary body's contact edge is not simply an arc centered about this point.

curve corresponds to the smallest r_f achieved, which is 0. Note, that for a given arm r_m, we may determine if a mechanism will not be able to actuate if the singularity zone of the socket and the swept singularity zone of the auxiliary body contact edge intersect. This would correspond to pushing the auxiliary body while in its singular zone, and then bottoming out in the sockets singular zone.

4.2 Design Comparison

For purposes of illustration, we show the differences in performance between a few different types of auxiliary body contact edge designs. We still restrict the designs to those where the auxiliary body rotates about a fixed point, and for sake of comparison, we keep the location of the pivot point fixed. Moreover, to isolate the benefit of auxiliary bodies, we restrict the socket's contact edge to a straight line.

Fig. 10 shows a comparison between a flat contact edge and shifted peaks. The peaks are shifted versions of one another, with the peaks either 10% (0.1 in the unitless coordinate system) of the total ball diameter to the left of center, directly below center, or 10% to the right of center. Given the location of the pivot point (significantly farther to the left), we firstly see that the flat edge does little to move the singularity away from the socket's singularity (at x =0). This is because the normal of the surface may only change by at most the rotation angle about the pivot, which is a small angle – only approximately 15° at its maximum. Moreover, the smoothness of the transition shows that any flat contact edge's r_f profile cannot shift the moment very much even with large rotations.

A peak design results in quite interesting behavior. The peak, which is actually rounded and not a discontinuity, leads to the normal direction changing very quickly as the contact moves over the peak. This in turn results in the moment very quickly changing and even flipping sign on different sides of the peak.

In fig. 10B, we see the effect of shifting the peak to the left. This design is not optimal for a few reasons. Firstly, its singular zone is quite near the socket's singular zone, so even when the auxiliary body would bottom out, there would still be very little moment. Moreover, when slightly to the left of the y axis, the auxiliary body's contact edge would result in a clockwise moment, but if contact were to occur on the socket instead, the moment induced would be counterclockwise. While the general case will be that the auxiliary body, when bottomed out, and the socket will have moments of different directions, the fact that both have their smallest moments so close to each other and are of differing sign could tend to make a mechanism "lock up" near the bottomed out position, even if the friction was quite low.

Fig. 10C shifts the peak directly under the contact point. While this appears to have similar issues as the peak in 10B, the fact that the moment induced by the auxiliary body's contact edge is much higher than the socket's near the socket singularity (shown by the blue-green color near (0, -0.4)) means that it would likely be difficult to reach the point where the aforementioned locking condition could occur.

Fig. 10D shows the peak shifted 10% to the right of center. While the singular curve of the auxiliary body is not far from the singular point of the socket, we note that the induced moment above the socket's singular point is now quite low. This type of design would likely work quite well in the case of low bearing and ball friction for reasons described in Section 2.2.2.

5. PROTYPE EVALUATION

As a proof of concept, a prototype of the joint design in fig. 10D using rigid auxiliary bodies (restored by rubber bands) and a prototype using deformable auxiliary bodies were manufactured. We call these concepts 1 and concept 2, respectively. Both concepts may be seen in fig 11. With both concepts, if the shaft is far from the vertical position, contacting the socket causes reconfiguration as the moment generated is quite high, and thus we are mostly concerned with the capacity for reconfiguration when the shaft is near vertical.

Figures 11A and 11B show concept 1. The articular bodies pivot about a pin, in the top of the socket, and are restored by the green and purple rubber bands, which have ends fixed to the socket (wrapped about a separate pin).

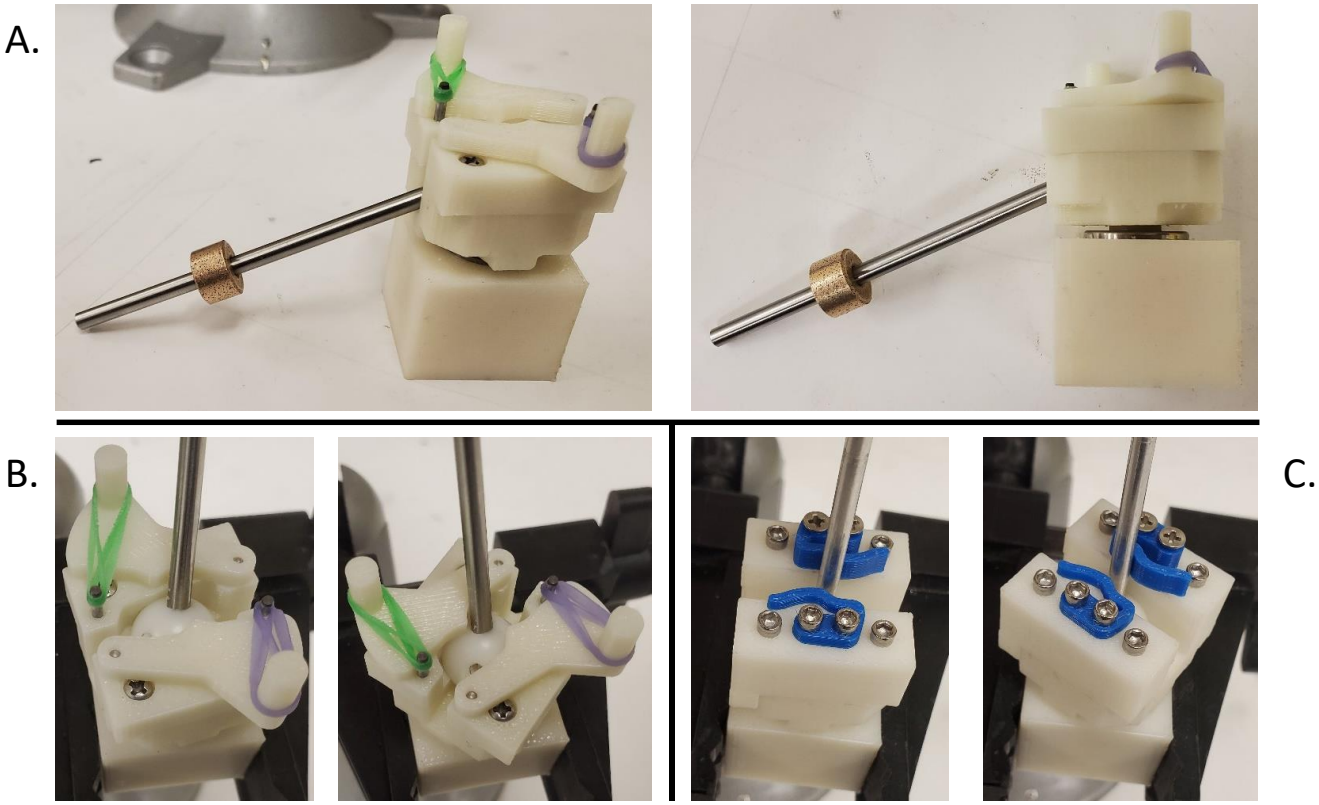

FIGURE 11. Prototype images. (A, Left) Concept 1, demonstrating its range of motion. Note the bronze bushing as an example distal bearing on the output shaft. (A, Right) A side view of concept 1 showing the proximal bearing located between the two blocks. (B, Left) Concept 1 auxiliary body maximally deflected, making initial contact with the socket's contact edge. Load on the shaft increases, leading to (B, Right), where the joint reconfigures, allowing the shaft to continue to move. (C, Left) Concept 2, with the deformable auxiliary bodies in blue. The left corresponds to an initial contact condition near the singularity of the auxiliary body. After increasing the force slightly, the body deforms, changing the contact normal, and then reconfigures, shown in C, right.

While actuating the joint using the distal bearing, reconfiguration occurs easily, whereas if we directly actuate the shaft and prevent free rolling, the joint can become stuck. This indicates there is a decent amount of friction between the ball and socket, which is to be expected of a 3D printed cavity.

Fig 11C shows a joint using deformable auxiliary bodies, where the deformation roughly approximates rotation about a fixed point. The design was found through heuristically optimizing the contact surface using geometric considerations, though an exhaustive discussion would be beyond the length constraints of this manuscript. We chose to use a deformable body design because placing the pivot point in the optimized location would be difficult given the material and strength properties.

Much of our analysis was nondimensionalized and only needed to consider unit forces. This made studying the effect of stiffness of the auxiliary body impossible, as there was no true force magnitude to relate to the displacement. To then examine the effect of stiffness, we increase the thickness of one of the auxiliary bodies (twice the thickness of its counterpart, likely twice the stiffness). When using the distal bearing, contact on either side of the joint leads to reconfiguration. When directly pinching the shaft, however, the thinner auxiliary body can bottom out and reconfiguration does not occur. The thicker body still manages to reconfigure when the shaft is directly actuated, however. This shows that while our analysis disregarded force magnitude, this approximation may sometimes fail if the forces involved are not high enough.

We note that the size of this joint is approximately 1 inch (~2.5 cm) on any side, leading to quite a compact joint. This kind of joint design may also easily be scaled in size or shrunk quite easily. The proximal and distal bearings can be incorporated into the base or platform structures if this type of joint was to be used in a parallel mechanism. The bearing friction and contact edge design leads to singularities being unreachable.

6. CONCLUSION

In this work, we present the design of a high range of motion ball and socket spherical joint using multiple contact edges. We introduce redundancy in the joint to allow for reconfiguration, and auxiliary bodies which may be deflected to shift the contact normal. We conduct a kinematic analysis to determine if a particular design can cause reconfiguration, and present prototypes of two exemplar designs. Future work will consider

ways in which to algorithmically optimize the contact geometry to generate maximally reconfiguring spherical joints. Additionally, experiments validating the intended function of the joints will be carried out, and the suitability of this joint in dynamic or high-speed situation will be assessed.

REFERENCES

[1] C. M. Gosselin, E. St. Pierre, and M. Gagné, “On the Development of the Agile Eye,” *IEEE Robotics and Automation Magazine*, vol. 3, no. 4, pp. 29–37, Dec-1996.

[2] D. Chablat and J. Angeles, “The Computation of All 4R Serial Spherical Wrists With an Isotropic Architecture,” pp. 1–12, 2007.

[3] R. Di Gregorio, “A new family of spherical parallel manipulators,” *Robotica*, vol. 20, no. June 2002, pp. 353–358, 2002.

[4] T. a. Hess-Coelho, “A Redundant Parallel Spherical Mechanism for Robotic Wrist Applications,” *J. Mech. Des.*, vol. 129, no. 8, p. 891, 2007.

[5] W. Chen, “A Novel Spherical Joint Designed for Metamorphic Mechanism,” *2008 IEEE Conf. Robot. Autom. Mechatronics*, pp. 976–981, 2008.

[6] E. F. Fichter, “A Stewart Platform- Based Manipulator : General Theory and Practical Construction,” *Int. J. Rob. Res.*, vol. 5, no. 2, pp. 157–182, 1986.

[7] P. Vischer and R. Clavel, “Argos: A Novel 3-DoF Parallel Wrist Mechanism,” *Int. J. Rob. Res.*, vol. 19, no. 1, pp. 5–11, 2000.

[8] F. Pierrot, C. Reynaud, and A. Fournier, “DELTA: a simple and efficient parallel robot,” vol. 8, no. 1990, pp. 105–109, 2020.

[9] R. Clavel, “DEVICE FOR THE MOVEMENT AND POSITIONING OF AN ELEMENT IN SPACE,” US 4,976,582, 1990.

[10] N. M. Bajaj, A. J. Spiers, and A. M. Dollar, “State of the Art in Artificial Wrists : A Review of Prosthetic and Robotic Wrist Design,” vol. 35, no. 1, pp. 261–277, 2019.

[11] L.-T. Schreiber and C. Gosselin, “Passively Driven Redundant Spherical Joint With Very Large Range of Motion,” *J. Mech. Robot.*, vol. 9, no. 3, p. 31014, 2017.

[12] G. L. Bieg, Lothar F., Benavides, “LARGE DISPLACEMENT SPHERICAL JOINT,” US 6,409,413, 2002.

[13] M. A. Peshkin and A. C. Sanderson, “Minimization of Energy in Quasi-Static Manipulation,” *Trans. Robot. Autom.*, vol. 5, no. 1, pp. 53–60, 1989.